Applied Physics Letters

Impact of roughness on heat conduction involving nanocontacts

Cite as: Appl. Phys. Lett. **119**, 161602 (2021); https://doi.org/10.1063/5.0064244
Submitted: 21 July 2021 • Accepted: 02 October 2021 • Published Online: 18 October 2021

Eloïse Guen, Pierre-Olivier Chapuis, Nupinder Jeet Kaur, et al.

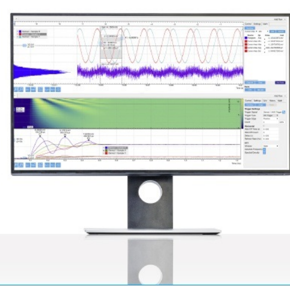

AIP Publishing

Applied Physics Letters ARTICLE scitation.org/journal/apl

Impact of roughness on heat conduction involving nanocontacts

Cite as: Appl. Phys. Lett. **119**, 161602 (2021); doi: 10.1063/5.0064244
Submitted: 21 July 2021 · Accepted: 2 October 2021 ·
Published Online: 18 October 2021

View Online Export Citation CrossMark

Eloïse Guen,[1] Pierre-Olivier Chapuis,[1] Nupinder Jeet Kaur,[2,3] Petr Klapetek,[2,3] and Séverine Gomés[1,a)]

AFFILIATIONS

[1]Centre d'Energétique et de Thermique de Lyon (CETHIL), UMR CNRS 5008, INSA Lyon, UCBL, Université de Lyon, Villeurbanne, France
[2]Czech Metrology Institute (CMI), Okružní 31, 638 00 Brno, Czech Republic
[3]CEITEC, Brno University of Technology, Purkyňova 123, 612 00 Brno, Czech Republic

[a)]Author to whom correspondence should be addressed: severine.gomes@insa-lyon.fr

ABSTRACT

The impact of surface roughness on conductive heat transfer across nanoscale contacts is investigated by means of scanning thermal microscopy. Silicon surfaces with the out-of-plane rms roughness of ~0, 0.5, 4, 7, and 11 nm are scanned both under air and vacuum conditions. Three types of resistive SThM probes spanning curvature radii over orders of magnitude are used. A correlation between thermal conductance and adhesion force is highlighted. In comparison with a flat surface, the contact thermal conductance can decrease as much as 90% for a microprobe and by about 50% for probes with a curvature radius lower than 50 nm. The effects of multi-contact and ballistic heat conduction are discussed. Limits of contact techniques for thermal conductivity characterization are also discussed.

Studying heat transfer across solid contacts with nano-scaled imperfections is crucial for many industrial applications involving micro-nano-components as in electronics.[1,2] Nanoscale roughness depends on fabrication processes, and its impact on the thermal transport across interfaces can even dictate the overall thermal resistance in nanosystems.[3] From a fundamental point of view, understanding thermal transport between two solids is important when the characteristic dimensions in the zone of thermal contact become comparable to key length scales, such as the mean free paths and the wavelengths of the energy carriers or the atomic distances of the materials in contact.[4–7]

Measurements are usually performed over areas with transverse characteristic sizes larger than the micrometer,[3] a scale where many nano-contacts may be present. There is hope that novel spatially resolved nanocharacterization methods based on scanning probe measurements (SPM) can allow for more systematic studies of the single contact (constriction), or at least of regions involving a limited number of contacts. Scanning thermal microscopy (SThM), i.e., SPM with a thermal sensor on the tip, allows for coupled nanoscale analyses of heat transfer and contact mechanics.[7] A previous SThM study of polished nanoscale contacts[4] suggested that roughness down to the atomic scale is important, underlining possible effects of thermal quantization across individual atomic-scale contacts. It is clear that surface roughness alters the mechanical contact at many different scales, inducing discontinuous and reduced multi-contacts, which in the majority of cases decreases the total thermal transfer.[8] Roughness also impacts the shape of the humidity-induced water meniscus located around the mechanical contacts, which can impact the heat transfer at the probe-sample contact.[9]

Here, thermal conductances between SThM tips of varying curvature radii and well-characterized rough silicon surfaces are determined, allowing to probe different contact scales. The total thermal contact radius and that due to the actual mechanical contact are discriminated while thermal results are correlated with adhesion forces. Thermal conductance is found to relate to the apparent contact radius at zero-force. It is also shown that the effect of roughness is comparable to that of an additional insulating layer, which can, in particular, be detrimental to SPM thermal measurements.

Three commercial resistive SThM probes were used: (1) the Wollaston wire probe[10] involving a 5-μm diameter wire with asperities at the apex, (2) the Pd probe[11] of Kelvin NanoTechnology where a palladium strip of curvature radius close to 100 nm is located at the apex, and the doped silicon (DS) probe[12] (AN300 thermal lever from Anasys Instruments) involving a ~10 nm curvature radius in silicon (see details in the supplementary material). In the so-called active mode, the probe resistive element is self-heated by the Joule effect in the dc regime using a constant electrical current. After calibration (details in supplementary material), control units based on Wheatstone bridges were used to monitor their mean temperature rise $\overline{\theta}_p$ and the electrical power P_{el} dissipated in the probe.

The samples consist of four silicon surfaces that have differing roughness parameters, prepared by anodic oxidation[13] and characterized by atomic force microscopy (AFM) (Fig. 1) by means of their root mean square roughness δZ_{RMS}, transverse correlation length l_c, and mean peak-to-peak distance (L_{RMS}). All these parameters allow each sample to be accurately characterized in both the perpendicular and parallel directions to the sample. One can note a correlation between the trends of δZ_{RMS} and l_c. In addition, an untreated sample of smooth silicon substrate ($\delta Z_{RMS} < 1$ nm) from the same batch is used as a reference.

To assess the impact of surface roughness, measurements based on (i) AFM vertical approach curves and (ii) images obtained by *xy* scanning were both made in ambient air and in primary vacuum (pressure $P \sim 0.28$ mbar), where the air contribution to the tip-sample transfer is eliminated. Results are provided as thermal conductances (see the supplementary material for details on protocols). Figure 2 reports on the decrease in thermal conductance (a) due to the global thermal transfer ($\Delta\overline{G}_{\text{global}}$) and (b) due to the tip jump to contact (ΔG^a_{mecha}), for the three probes and both types of experimental conditions. Mechanical contacts form after the jump, possibly with the water meniscus. We note strong differences between the behaviors with the different probes. When sample roughness increases, $\Delta\overline{G}_{\text{global}}$ decreases by 30% for the Wollaston probe [Fig. 2(a-A)] and by about 10% for the Pd probe [Fig. 2(a-B)]. For the DS probe, $\Delta\overline{G}_{\text{global}}$ remains constant [Fig. 2(a-C)]. The observed conductance decreases are the signature of the decrease in heat conduction through the mechanical contact, as the air heat transfer taking place over a $\sim$ micrometric zone is not expected to vary much when roughening the surface. For the largest probe [Wollaston, Fig. 2(a)], it is found that the heat conduction by mechanical contact (solid–solid and water meniscus) on a flat surface represents 20% of the overall transfer. This thermal transfer can almost be suppressed by roughening the surface (decrease by 95%) [Fig. 2(b-A)]. The overall decrease can be larger than 20%, so heat transfer through air is also slightly reduced, probably due to an effective tip-sample distance larger in the rough case. For the roughest sample, the mechanical contact accounts for only 2% of the overall heat transfer. In contrast, thermal transfer across mechanical contact accounts for less than 1% of the overall transfer on a flat surface for the smallest tip apex [DS probe, Fig. 3(c)]. Although this transfer decreases with increased roughness, it has no visible effect on the measured overall transfer. Finally, the Pd probe, which has intermediate dimensions, exhibits an intermediate behavior [Figs. 3(a-B)–(b-B)]. On a flat surface, about 11% of the global transfer is made through mechanical contact. With the increase in roughness, this transfer decreases by up to 30%, resulting in a 5%–10% decrease on the overall signal measured. These results on thermal transfer across the first contact during an approach curve of the SThM tip on the sample show that surface roughness results in a decrease in the heat transfer across the contact, presuming a decrease in the probe-sample contact area. Analysis of thermal images of samples leads to the same conclusion (see the supplementary material for images).

Measurements of the adhesion forces[14] performed with the three probes on the rough samples are consistent with this observation. Figure 3 shows the thermal conductance ΔG^a_{mecha} as a function of the average value of the adhesion force (F_{ad}) measured for each SThM probe. When sample roughness increases, the adhesion force decreases by up to 97%, about 30% and 50%, respectively, for the Wollaston, Pd and DS probes. This underlines the correlation between the quality of the probe-sample contact and the heat transfer across it. Roughness significantly deteriorates the quality of the probe-sample contact and, thus, the thermal transfer associated with mechanical contact. The effect seems more pronounced for the Wollaston microprobe than for the nanoprobes. This can be explained by the roughness of the metallic microfilament:[15] The Wollaston probe-planar sample contact is made by a multitude of small contacts, and the number of which is decreased

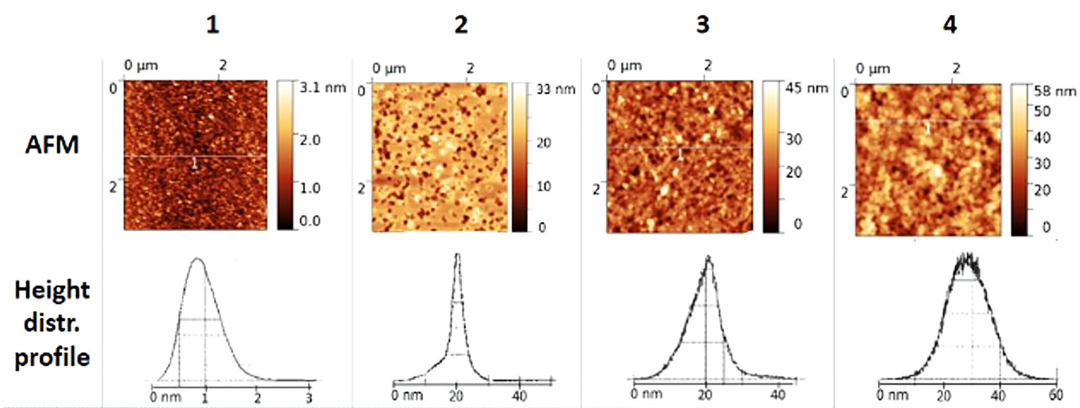

	1	2	3	4
δZ_{RMS}	0.5 nm	4 nm	7 nm	11 nm
l_c	38 nm	58 nm	65 nm	86 nm
L_{RMS}	126 nm	137 nm	214 nm	215 nm

FIG. 1. Topographic images obtained from AFM, distributions of the associated heights and roughness parameters (δZ_{RMS}, l_c and L_{RMS}) for the four rough samples.

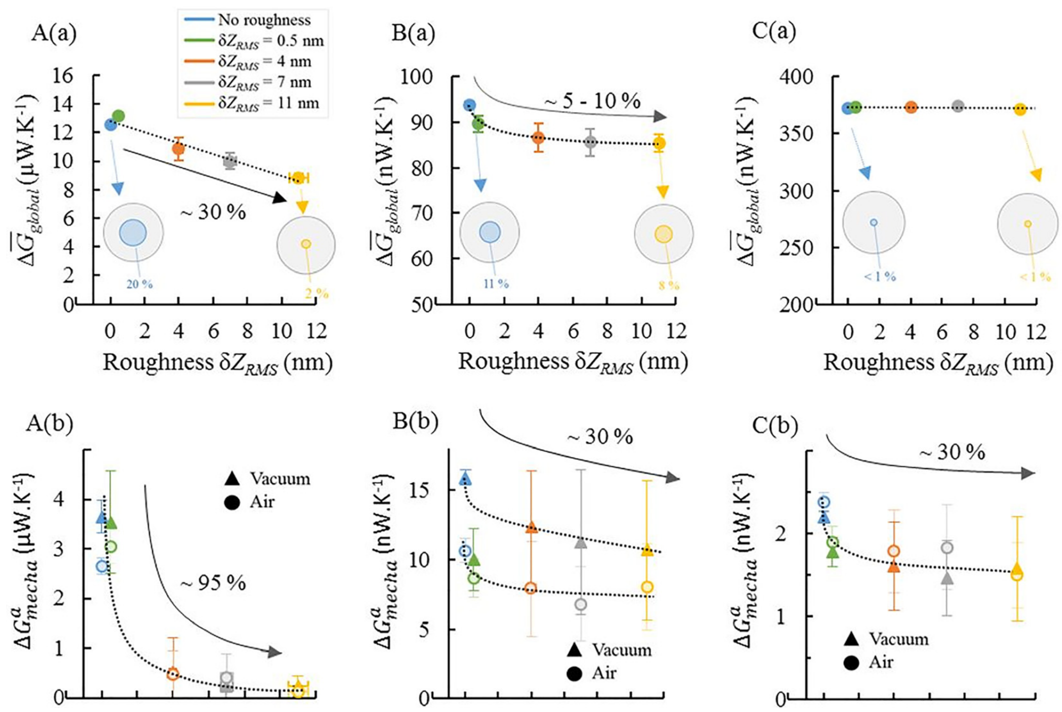

FIG. 2. Measured global (a) and mechanical contact-related (b) thermal conductances according to the Si roughness, for the Wollaston (A), Pd (B), and doped Si (C) probes. (a) refer only to air measurements. Inset schematics represent the percentage of the mechanical contact heat transfer in the global heat transfer between probe and sample. For vacuum measurements $\Delta\overline{G}_{global} = \Delta G^a_{mecha}$. Error bars represent dispersion of the measurements.

when the surface becomes rough, resulting in a significant decrease in the total contact area. Measurements with nanoprobes are less impacted for the studied roughness range.

An upper bound for the curvature radius R at the contact can be obtained by neglecting the influence of the water meniscus on adhesion (note that we do not expect the water meniscus to be predominant for heat transfer[9–15]). R is determined from the adhesion force, measured when retracting the probe from the sample, by using the mechanical model of Rabinovich *et al.*[16,17] This model considers a rough surface with periodic peak-to-peak distance L_{RMS} and mean

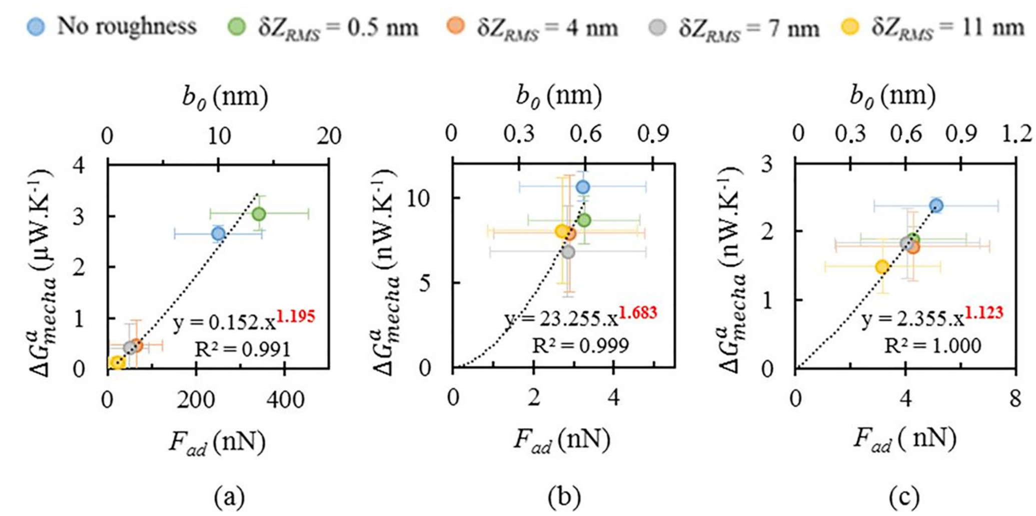

FIG. 3. Thermal conductance due to mechanical contact as a function of the adhesion force (F_{ad}) and corresponding contact radii for experiments performed in air conditions on the rough samples with (a) the Wollaston probe, (b) the Pd probe and (c) the DS probe.

out-of-plane deviation δZ_{RMS} associated with hemispherical asperities of curvature radius $r = f(\delta Z_{RMS}, L_{RMS})$,

$$F_{ad} = \frac{A_H.R}{6.H_0^2} \frac{1}{\left(1 + 58.14\,\frac{R\,\delta Z_{RMS}}{L_{RMS}^2}\right).\left(1 + 1.817\,\frac{\delta Z_{RMS}}{H_0}\right)^2}, \qquad (1)$$

where $A_H \sim 2.65 \times 10^{-19}$ J is the Hamaker constant and $H_0 = 0.3$ nm is the minimum separation distance between the tip apex and the asperity. Using this expression, one finds $R = 9 \pm 2$ nm for the DS probe in accordance with previous estimate,[12] $R = 6.4 \pm 0.5$ nm for the Pd probe, which is ten to five times lower than the values announced by the provider.[12] This difference could be understood as a contact considered to be made through an asperity at the apex of the tip. For the Wollaston probe that is the largest and roughest probe, R values are very dispersed and the mean is around 450 nm as found in Ref. 15. Equation (1), which assumes that the surface is rougher than the probe ($R > L_{RMS,}\ \delta Z_{RMS}$), could, therefore, be applicable for the Wollaston probe but is only approximate for the two other probes. Adding the Derjaguin–Müller–Toporov (DMT) model for the sphere-plane configuration,[18] we can determine, for each surface, a lower bound for the contact radius b_0 when zero force is applied,

$$b_0 = \sqrt[3]{\frac{1}{E^*}\frac{R.r}{R+r}F_{ad}}, \qquad (2)$$

where r is the curvature radius of rough surface asperities and E^* is the generalized Young modulus. Figure 3 provides this quantity for the various probes. For the Wollaston probe, ΔG^a_{mecha} is found proportional to $b_0^{1.2}$, for the Pd nanoprobe to $b_0^{1.6}$ and for the DS probe to $b_0^{1.1}$. It is known that when $\Delta G^a_{mecha} \propto b_0$ heat transfer is diffusive and that $\Delta G^a_{mecha} \propto {b_0}^2$ for a ballistic[19] or thermal-boundary limited (Kapitza) transfer. The oxide layer that is present on the surface of samples and probably on the resistive elements of the probes can be involved in this interfacial thermal resistance. For the three probes, the exponent is larger than 1, which suggests that thermal transfer is not only diffusive. Let us note, however, that b_0 values are well below the phonon average mean free path of Si (around 250 nm) so that an exponent closer to 2 would be expected. The role of water meniscus on adhesion, which is here neglected, could explain the difference with such value. A generalization of Eq. (1) to arbitrary values of R, which would include contact of the probes' sides with the samples, would be useful to clarify these observations.

It is interesting to analyze the heat transfer reduction in light of the usual SThM measurement process, which involves first a calibration with samples of well-known thermal conductivity with surfaces as flat as possible. Figure 4 provides such a calibration curve, which underlines the lack of sensitivity for large thermal conductivity. Most importantly, it highlights that using the average value of ΔG^a_{mecha} for a rough sample of unknown thermal conductivity would lead to determining a thermal conductivity much lower than the correct value (see red arrow), as if an insulating body was present below the surface. Using the upper values of the conductance range may be better (possibly also for the calibration curve) but induces also uncertainty. As a consequence, a detailed analysis of roughness is essential prior to SThM thermal-conductivity determination from the contact.

In conclusion, we have measured thermal conductances across micro- to nanocontacts by means of SThM probes on Si samples. For roughness δZ_{RMS} close to 10 nm, the decrease in contact thermal conductance can reach as much as 90% at a microcontact and about 50% at nanocontacts. In all cases, surface roughness strongly alters the mechanical contact, resulting in most cases in multi-contacts reducing the apparent contact radius. It is found that heat transfer is not only diffusive, but that ballistic or boundary-limited heat conduction can also be involved. Finally, we demonstrate that sample roughness can completely distort the analysis of SThM measurements when estimating thermal conductivity of materials. It will be needed to study the effect of roughness on materials covering the whole thermal conductivity range in order to be able to analyze correctly the thermal data. Another pending issue is that current mechanical models consider only the mechanical properties of solid materials, so the water meniscus and its contact radius deserve to be further investigated.

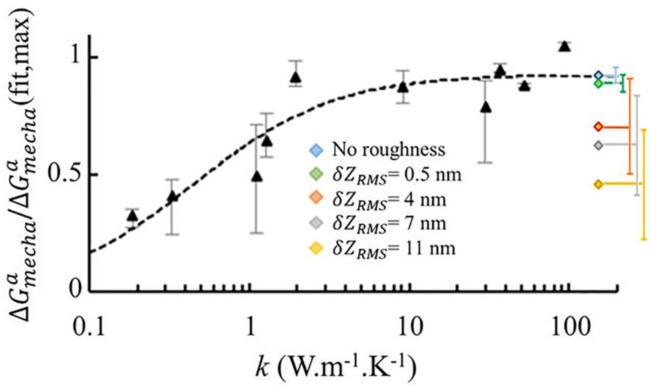

FIG. 4. Normalized thermal conductance across contact as a function of apparent sample thermal conductivity k for both reference and rough samples (Pd probe operated in vacuum). The dashed black line is a calibration curve obtained from average thermal conductances of bulk reference materials with roughness as low as possible (black dots) with a different probe (see the supplementary material for explanations).

See the supplementary material for further details on SThM probe and sample characterizations, SThM images, and protocols.

The research leading to these results has received funding from the European Union Seventh Framework Programme FP7-NMP-2013-LARGE-7 under Grant Agreement No. 604668.

DATA AVAILABILITY

The data that support the findings of this study are available from the corresponding author upon reasonable request.

REFERENCES

[1] D. G. Cahill, P. V. Braun, G. Chen, D. R. Clarke, S. Fan, K. E. Goodson, P. Keblinski, W. P. King, G. D. Mahan, A. Majumdar, H. J. Maris, S. R. Phillpot, E. Pop, and L. Shi, "Nanoscale thermal transport. II. 2003–2012," Appl. Phys. Rev. **1**(1), 011305 (2014).
[2] L. Shi, C. Dames, J. R. Lukes, P. Reddy, J. Duda, D. Cahill, J. Lee, A. Marconnet, K. E. Goodson, J.-H. Bahk, A. Shakouri, R. S. Prasher, J. Felts, W. P. King, B. Han, and J. C. Bischof, "Evaluating broader impacts of nanoscale thermal transport research," Nanoscale Microscale Thermophys. Eng. **19**(2), 127–165 (2015).

[3]A. Giri and P. E. Hopkins, "A review of experimental and computational advances in thermal boundary conductance and nanoscale thermal transport across solid interfaces," Adv. Funct. Mater. **30**, 1903857 (2020).
[4]B. Gotsmann and M. Lantz, "Quantized thermal transport across contacts of rough surfaces," Nat. Mater. **12**(1), 59–65 (2013).
[5]A. Majumdar and B. Bhushan, "Role of fractal geometry in roughness characterization and contact mechanics of surfaces," J. Tribol. **112**(2), 205 (1990).
[6]A. Majumdar and B. Bhushan, "Fractal model of elastic-plastic contact between rough surfaces," J. Tribol. ASME **113**(1), 1–11 (1991).
[7]S. Gomès, A. Assy, and P.-O. Chapuis, "Scanning thermal microscopy: A review," Phys. Status Solidi A **212**(3), 477–494 (2015).
[8]H. Fischer, "Quantitative determination of heat conductivities by scanning thermal microscopy," Thermochim. Acta **425**(1–2), 69–74 (2005).
[9]A. Assy and S. Gomès, "Experimental investigation of capillary forces at nanosized contacts through heated AFM cantilever probe," Nanotechnology **26**(35), 355401 (2015).
[10]R. B. Dinwiddie, R. J. Pylkki, and P. E. West, "Thermal conductivity contrast imaging with a scanning thermal microscope," in *Proceedings of the 22nd International Conference on Thermal Conductivity, Tempe AZ, 1993*, edited by T. W. Wong (Technomic Publishing Co., 1994), pp. 668–677.
[11]P. S. Dobson, J. M. Weaver, and G. Mills, "New methods for calibrated scanning thermal microscopy (SThM)," *Sensors* (IEEE, 2007), pp. 708–711.
[12]P. Tovee, M. Pumarol, D. Zeze, K. Kjoller, and O. Kolosov, "Nanoscale spatial resolution probes for scanning thermal microscopy of solid-state materials," J. Appl. Phys. **112**(11), 114317 (2012).
[13]J. Zemek, K. Olejník, and P. Klapetek, "Photoelectron spectroscopy from randomly corrugated surfaces," Surf. Sci. **602**(7), 1440–1446 (2008).
[14]B. N. Persson and M. Scaraggi, "Theory of adhesion: Role of surface roughness," J. Chem. Phys. **141**(12), 124701 (2014).
[15]A. Assy, S. Lefèvre, P. O. Chapuis, and S. Gomès, "Analysis of heat transfer in the water meniscus at the tip-sample contact in scanning thermal microscopy," J. Phys. D: Appl. Phys. **47**(44), 442001 (2014).
[16]Y. I. Rabinovich, J. J. Adler, M. S. Esayanur, A. Ata, R. K. Singh, and B. M. Moudgil, "Capillary forces between surfaces with nanoscale roughness," Adv. Colloid Interface Sci. **96**(1–3), 213–230 (2002).
[17]Y. I. Rabinovich, J. J. Adler, A. Ata, R. K. Singh, and B. M. Moudgil, "Adhesion between nanoscale rough surfaces. I. Role of asperity geometry," J. Colloid Interface Sci. **232**(1), 10–16 (2000).
[18]B. V. Derjaguin, V. M. Muller, and Y. P. Toporov, "Effect of contact deformation on the adhesion of elastic solids," J. Colloid Interface Sci. **53**(2), 314–326 (1975).
[19]R. A. Prasher, T. Tong, and A. Majumdar, "Diffraction-limited phonon thermal conductance of nanoconstrictions," Appl. Phys. Lett. **91**(14), 143119 (2007).